Pressure-Modulated Activation Energy as a Unified Descriptor of Mechanical Behavior in Metallic Glass

Huanrong Liu(刘桓荣)[1], Jian Li(李健)[2*], Shan Zhang(张珊)[2,1*], and Pengfei Guan(管鹏飞)[2,1*]

[1]*Beijing Computational Science Research Center, Beijing 100193, China*
[2]*Advanced Interdisciplinary Science Research Center (AiRCenter) , Ningbo Institute of Materials Technology and Engineering, Chinese Academy of Sciences, Ningbo 315201, China*

(Received 24 October 2025; accepted manuscript online 25 November 2025)

The functional properties of glasses are governed by their formation history and the complex relaxation processes they undergo. However, under extreme conditions, glass behaviors are still elusive. In this study, we employ simulations with varied protocols to evaluate the effectiveness of different descriptors in predicting mechanical properties across both low- and high-pressure regimes. Our findings demonstrate that conventional structural and configurational descriptors fail to correlate with the mechanical response following pressure release, whereas the activation energy descriptor exhibits robust linearity with shear modulus after correcting for pressure effects. Notably, the soft mode parameter emerges as an ideal and computationally efficient alternative for capturing this mechanical behavior. These findings provide critical insights into the influence of pressure on glassy properties, integrating the distinct features of compressed glasses into a unified theoretical framework.

DOI: 10.1088/0256-307X/43/1/010602 CSTR: 32039.14.0256-307X.43.1.010602

Metallic glasses (MGs) find wide applications[1–4] owing to their unique disordered structures derived from rapidly quenched melts. Unlike crystalline materials, MGs possess a homogeneous amorphous microstructure and are free of well-defined defects.[5–7] As a result, directly parsing the structure-property relationship remains challenging. An alternative way to decode the interplay relies on the protocol history, which captures not only structural features but also the dynamical trajectory.[8,9] Prior experiments and simulations have demonstrated that properties of MGs can be substantially enhanced by controlling glass-forming protocols, which involve thermal or mechanical treatment. For instance, annealing treatment allows MGs to relax into a lower-energy state, while high-pressure (HP) treatment induces a rejuvenated state characterized by enhanced orderliness, compressed volume, and elevated energy.[10–12] Notably, HP treated MGs exhibit significant enhancements in strength and ductility,[11] polymorphic transitions,[13,14] and devitrifications.[15] Conceptually, pressure-induced behaviors are associated with features from the potential energy landscape (PEL).[16,17] However, a sound framework extending these PEL-related models after pressure release remains scarce. In this study, the primary goal is to extend the powerful PEL descriptor[18] to HP regimes. To this end, we quantitatively investigate the interplay between descriptors and mechanical properties—both before and after pressure release.

$Cu_{50}Zr_{50}$ configurations with 4000 atoms were prepared across a wide range of cooling rate-pressure combinations. For all molecular dynamics simulations, we adopted the realistic embedded-atom method interatomic potential[19] and applied periodic boundary conditions. As shown in Fig. 1(a), the preparation protocol follows: (i) bathing the glass-forming liquid at 2000 K with a specific hydrostatic pressure ($P = 0$ to 20 GPa) and quenching the liquid to 1 K at four different cooling rates, from 10^{10} K/s up to 10^{13} K/s. The samples generated here are referred to as HP samples; (ii) unstraining the configuration to zero pressure within 10 ns. The samples after pressure release are referred to as pressure-released (RP) samples. The symbol "P" of RP samples denotes the pressure level prior to stage (ii), as illustrated in Fig. 1(a). During preparation, the HP and RP samples share identical compositions and cooling rates, with pressure serving as the sole variable that drives differences in their microstructure and properties, including density, atomic packing behavior, and mechanical properties. Additionally, we employed the activation-relaxation technique (ART)[20–22] to acquire the statistical profiles of saddle points. Each randomly selected atom in the generated sample triggers 10 ART searches. In each perturbation, we randomly chose the direction and fixed the displacement at 0.5 Å. A convergence criterion for saddle point identification was set such that the system was deemed to have converged to a saddle point when the atomic forces fell below 0.05 eV/Å. Following the exclusion of failed and redundant saddle point searches,[21] each HP and RP sample yielded approximately 16000 and 24000 perturbation processes, respectively. The discrepancy stems from a qualitative change in the PEL topology under high pressure, where the final states of two distinct zero-pressure minimum energy paths (MEPs) may collapse

*Corresponding authors. Email: lijianalpha@nimte.ac.cn; zhangshan@nimte.ac.cn; pguan@csrc.ac.cn
© 2026 Chinese Physical Society and IOP Publishing Ltd. All rights, including for text and data mining, AI training, and similar technologies, are reserved.

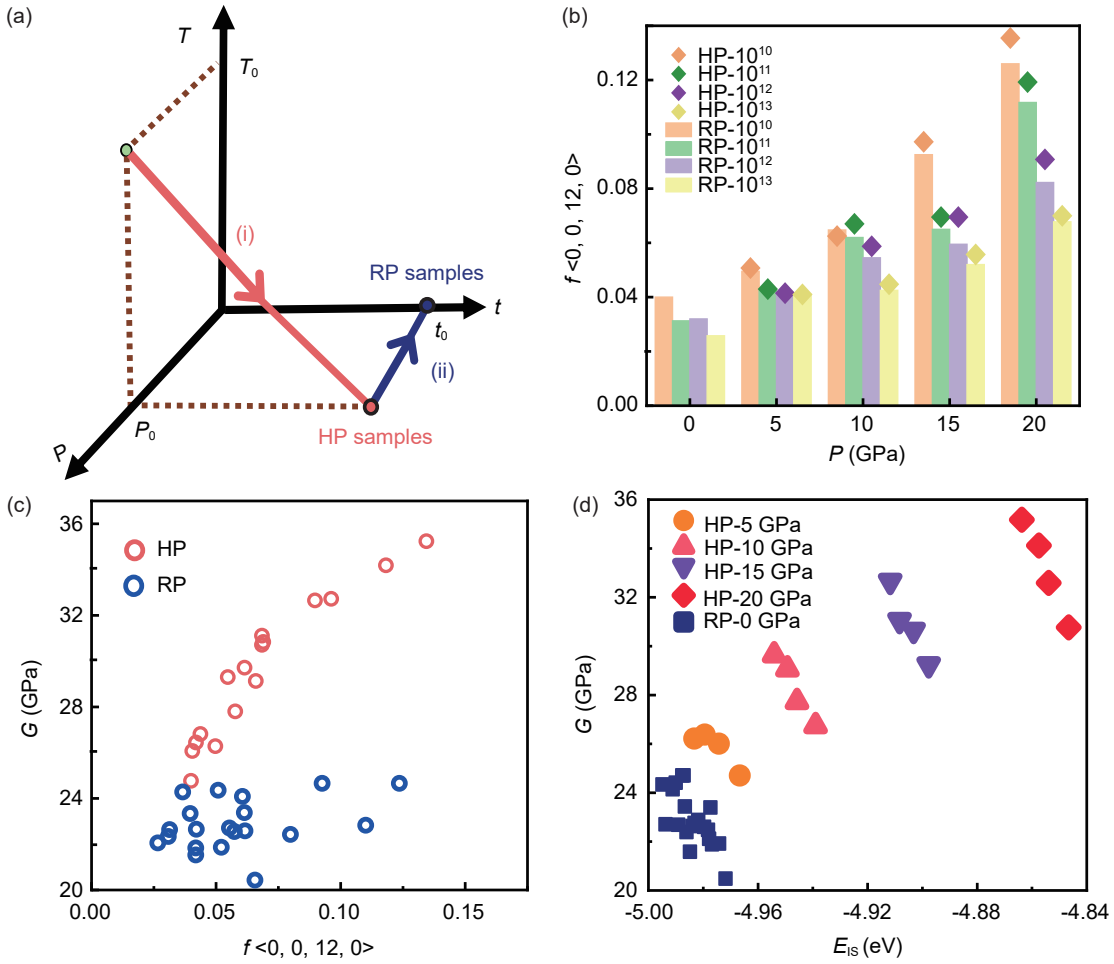

Fig. 1. (a) Schematic diagram of protocols for preparation of HP and RP samples. (b) Pressure-cooling rate dependence of icosahedral proportion (marked by colored rhombus) and its residual profile after pressure release (shown in histograms). (c) Relationship between shear modulus and icosahedral proportion in HP (red spheres) and RP (blue spheres) samples. (d) Relationship between shear modulus and energy of inherent structures in HP samples at 5 GPa (yellow spheres), 10 GPa (pink triangles), 15 GPa (purple inverted triangles), and 20 GPa (red rhombus), and in RP samples (blue squares).

into the same basin.

The limitation of icosahedral proportion,[23] which generally fails to describe protocol-related pressure dependence, is identified. As depicted in Fig. 1(b), although the icosahedral proportion can partially distinguish HP samples subjected to different pressures, the residual difference after pressure release still remains. As a result, the icosahedral proportion perfectly captures the variation of shear modulus of HP samples but fails to effectively distinguish RP samples, as seen in Fig. 1(c). This highlights the challenges in directly inferring pressure-modulated correlations via statistical analysis of icosahedrons. A similar trend emerges when examining configurational energy. Figure 1(d) reveals that both the shear modulus (G) and inherent structure energy (E_{IS})[24,25] of HP samples increase with HP preparation. While HP samples display linear relationships with identical slopes over a range of pressures, RP samples, by contrast, show dispersion in their linearity attributed to residual effects from the HP regime.

This dilemma offers a novel perspective to decouple the pressure effects by two-level systems,[5,26,27] which correlate glass properties with the transition events instead of energy levels.[28] Following this idea, we have previously established a linear connection between G and E_{IS} without pressure treatment through activation spectra.[21] The question then arises: how does this linear relationship change with HP protocols?

To answer the question, we analyzed the activation events under distinct pressures. Figure 2 presents detailed PEL profiles of HP and RP samples with different cooling rates and barostat conditions. As shown in Fig. 2(a), the peak of the E_A spectrum shifts toward larger values with increasing pressure, while the corresponding peak in RP samples remains unchanged. Conceptually, increasing pressure induces denser and more ordered packing with a higher energy barrier than that of RP samples, thus causing the peak shift. Additionally, the proportion of atoms with low activation energy increases with the cooling rate, irrespective of pressure release. The newly emergent activations also significantly bias the skewness of the distributions [see Fig. S1 of the Supplementary Materials (SM)].

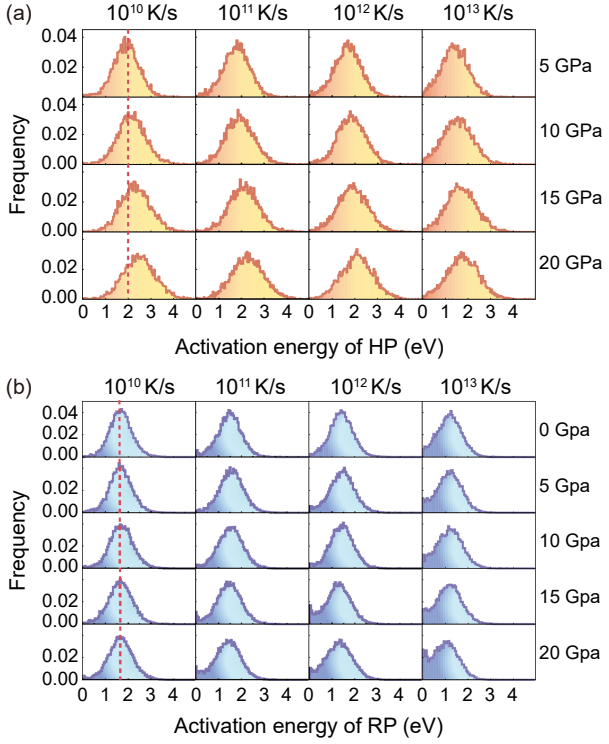

Fig. 2. Activation energy distributions of (a) HP and (b) RP samples with distinct pressures and cooling rates. Vertical panels represent the barostat condition dependence, and horizontal ones display the cooling rate dependence.

However, as disclosed by Fig. 2(b), the distribution tail of HP samples is less pronounced, indicating that the low-energy activation events of HP metabasins are rare and suggesting a more kinetically stable structure in HP control protocols. No significant difference is observed in the pair correlation (see Fig. S2 of the SM).

With the prior knowledge about activation profiles of HP and RP samples, we can delve deeper into the corresponding mechanical response. Figure 3(a) illustrates the correlation between the shear modulus (G) and the arithmetic mean of $E_{\rm A}$ spectrum ($\bar{E}_{\rm A}$) for HP and RP samples. The correlation is roughly linear with large dispersions under different pressures. After scaling $\bar{E}_{\rm A}$ with a pressure-modulated correction $\Delta\bar{E}_{\rm A,P}$, shear modulus G and generalized activation energy $\bar{E}_{\rm A}+\Delta\bar{E}_{\rm A,P}$ collapse to a clear linear relationship in Fig. 3(b), as shown by the black straight line representing the following equation:

$$G = k_1(\bar{E}_{\rm A}+\Delta\bar{E}_{\rm A,P})+G_0\,, \tag{1}$$

where $k_1 = 5.76$, $G_0 = 14.6$ GPa. The intercept G_0 signifies the extrapolated value of shear modulus when approaching the nearly constant loss.[29–31] The extrapolated shear modulus is consistent with that of instantly quenched samples. The correction $\Delta\bar{E}_{\rm A,P}$ shows linearity fitting with pressure P: $\Delta\bar{E}_{\rm A,P} = 0.05P$, as shown in Fig. 3(c). Compared with conventional descriptors based on static configurations, the activation energy descriptor

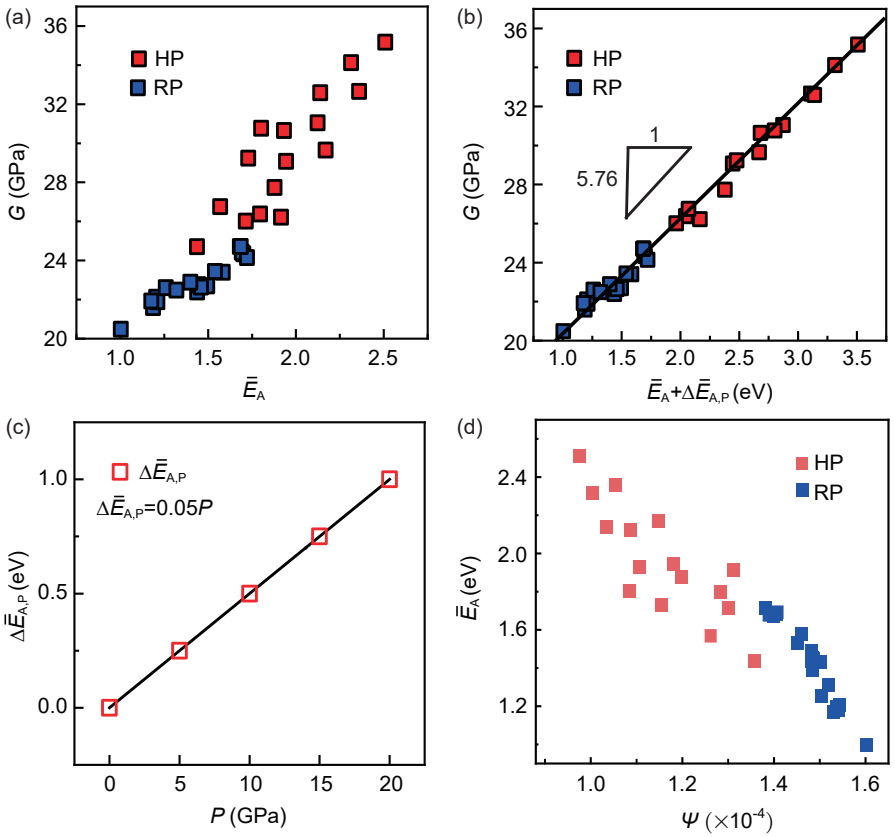

Fig. 3. The (a) raw and (b) scaled correlations between the shear modulus G and the arithmetic mean activation energy $\bar{E}_{\rm A}$. The slope of the scaled line is indicated by the triangle. (c) The pressure dependence of activation energy correction $\Delta\bar{E}_{\rm A,P}$. (d) The correlation between soft mode parameter ψ and activation energy $\bar{E}_{\rm A}$ of HP and RP samples.

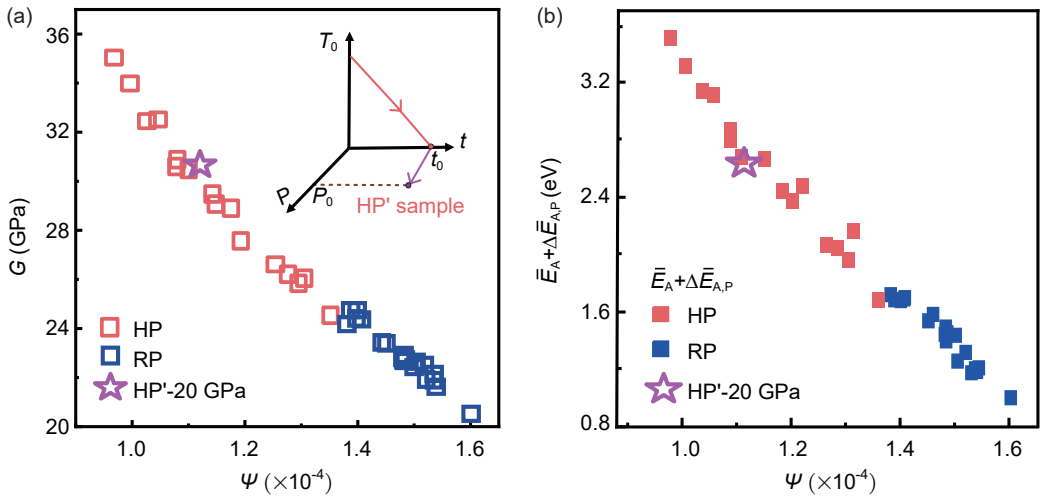

Fig. 4. (a) Correlation between soft mode parameter ψ and shear modulus G. The inset provides the protocol of HP' sampling. (b) Correlation between soft mode parameter ψ and corrected activation energy $\bar{E}_{\rm A} + \Delta\bar{E}_{\rm A,P}$.

unifies mechanical properties under different protocols.

On the one hand, owing to the high computational cost of activation spectra (see SM for more details), there is an urgent need for alternative descriptors that acquire robust linear mapping. On the other hand, the strong linearity of corrections motivates us to examine its generality for other glass properties. Here we choose the soft mode parameter ψ related to low-frequency vibrational modes.[32,33] However, according to the raw scatter plot in Fig. 3(d), a similar failure (of the correlation mentioned earlier) is observed in the linear fitting of HP samples. It indicates that the dispersion in the HP regime is intrinsic and that correction of pressure effects is needed.

By contrast, figure 4(a) clearly reveals that the soft mode parameter is a robust descriptor for shear modulus, enabling it to unify both HP and RP samples within the same linear framework. Additionally, in Fig. 4(b), the soft mode parameter serves as an alternative, consistent with the linearity shown in Figs. 4(a) and 3(b). The result strongly suggests that it is possible to mitigate the computational complexity of barrier explorations, with more efficient vibrational mode calculations.[33] To validate the intrinsic nature of pressure-modulated corrections, we also conducted another protocol replica to HP states, which involves an unstrained quench in melts and an athermal compression afterwards. The result is referred to as HP in Figs. 4(a) and 4(b). The linearity after corrections is consistent with other HP and RP samples, depicting the path-independent feature of pressure-modulated activation energy. We deduce that the correction in HP regimes originates from the compressed boundary. That is, strained systems naturally outperform unstrained ones in relaxing into the PEL bottom, which is consistent with the distinguishable inherent energy distributions of HP and RP samples (see Figs. S3 and S4 of the SM). Additionally, the constant slope of corrections ($0.05\,\text{eV/GPa} = 8\,\text{Å}^3$) indicates that the volume modulation of energy barrier is stationary, characterizing the volumetric response inherited from constraints. Furthermore, the results (see Fig. S5 of the SM) clearly exclude any interplay with local structural orders, highlighting a larger configurational space with diverse structural indicators.

In summary, we propose a unified descriptor from the landscape spectrum of MGs. For computational convenience, we also recommend the soft mode parameter as the optimal alternative to pressure-modulated activation energy. The generalized activation energy can be directly correlated with the shear modulus and soft mode parameter, both before and after pressure release. Conceptually, the strong linearity after correction originates from the variation of MEPs of tunneling states,

$$\Delta\bar{E}_{\rm A,P} = \frac{1}{N_{\rm P}} \sum_{i=1}^{N_{\rm P}} \left[E^i_{\rm A}(P=0) - E^i_{\rm A}(P) \right], \qquad (2)$$

where $N_{\rm P}$ represents the number of existing MEPs. In consistence with the seminal work,[34] the constant response volume ($\approx 8\,\text{Å}^3$) is sufficient to induce significant tortuosity in MEPs, yet too small to drive collective rearrangement.

Notably, as shown in Fig. 2(b), pressure release induces newly emergent low-barrier activations, mirroring the effects of strain-controlled loading. To avoid triggering structural instabilities (for example, shear bands), athermal pressure release is implemented via instant affine transformations of the simulation box. This transient expansion more effectively drives qualitative changes in the PEL topology, ultimately giving rise to the observed low-barrier activations.

As of now, decoding the HP landscape spectrum of glasses is still a great challenge. However, our work presents a robust navigator in such unknown complexity, mapping different pressure regimes into unstrained ones. The broadband spectrum of HP soft modes also enlarges the conventional structure-property dataset[35,36] informed by machine learning. With the assistance of general-purpose machine learning force fields,[37,38] pressure modulations on activation spectra can serve as the fingerprint of distinct disorder, deepening our understanding of hidden glassy patterns beyond local and noisy features.

Acknowledgments. This work was supported by the National Natural Science Foundation of China (Grant Nos. T2325004 and 52161160330), Advanced Materials-National Science and Technology Major Project (Grant No. 2024ZD0606900), and the Talent Hub for "AI+ New Materials" Basic Research. We acknowledge the computational support from the Beijing Computational Science Research Center (CSRC). S.Z. acknowledged the National Natural Science Foundation of China (Grants No. 12504233). J.L. acknowledged the Key Research and Development Program of Ningbo (Grant No. 2025Z088).

References

[1] Wang W H, Dong C, and Shek C H 2004 *Mater. Sci. Eng.: R: Rep.* **44** 45
[2] Inoue A 2000 *Acta Mater.* **48** 279
[3] Inoue A and Takeuchi A 2011 *Acta Mater.* **59** 2243
[4] Schuh C A, Hufnagel T C, and Ramamurty U 2007 *Acta Mater.* **55** 4067
[5] Ciarella S, Khomenko D, Berthier L, Mocanu F C, Reichman D R, Scalliet C, and Zamponi F 2023 *Nat. Commun.* **14** 4229
[6] Bera A, Zaccone A, and Baggioli M 2025 *Nat. Commun.* **16** 5990
[7] Hu Y C and Tanaka H 2025 *Nat. Commun.* **16** 5321
[8] Sastry S, Debenedetti P G, and Stillinger F H 1998 *Nature* **393** 554
[9] Grigera T S, Martín-Mayor V, Parisi G, and Verrocchio P 2003 *Nature* **422** 289
[10] Miyazaki N, Wakeda M, Wang Y J, and Ogata S 2016 *npj Comput. Mater.* **2** 16013
[11] Yamada R, Shibazaki Y, Abe Y, Ryu W, and Saida J 2019 *NPG Asia Mater.* **11** 72
[12] Shen J, Cornet A, Ronca A *et al.* 2025 *Sci. Adv.* **11** eadz7406
[13] Li L, Luo Q, Li R, Zhao H, Chapman K W, Chupas P J, Wang L, and Liu H 2017 *Sci. Rep.* **7** 46762
[14] Sheng H W, Liu H Z, Cheng Y Q, Wen J, Lee P L, Luo W K, Shastri S D, and Ma E 2007 *Nat Mater* **6** 192
[15] Zeng Q, Sheng H, Ding Y, Wang L, Yang W, Jiang J Z, Mao W L, and Mao H K 2011 *Science* **332** 1404
[16] Debenedetti P G and Stillinger F H 2001 *Nature* **410** 259
[17] Fan Y, Iwashita T, and Egami T 2017 *Nat. Commun.* **8** 15417
[18] Li H, Xiao H, Egami T, and Fan Y 2024 *Mater. Today Phys.* **49** 101582
[19] Cheng Y Q and Ma E 2011 *Prog. Mater Sci.* **56** 379
[20] Mousseau N, Béland L K, Brommer P, Joly J F, El-Mellouhi F, Machado-Charry E, Marinica M C, and Pochet P 2012 *Journal of Atomic, Molecular, and Optical Physics* **2012** 925278
[21] Zhang S, Liu C, Fan Y, Yang Y, and Guan P 2020 *J. Phys. Chem. Lett.* **11** 2781
[22] Fan Y, Iwashita T, and Egami T 2017 *Nat. Commun.* **8** 15417
[23] Wang B, Shang B S, Gao X Q, Wang W H, Bai H Y, Pan M X, and Guan P F 2016 *J. Phys. Chem. Lett.* **7** 4945
[24] Liu C, Guan P, and Fan Y 2018 *Acta Mater.* **161** 295
[25] Lacks D J and Osborne M J 2004 *Phys. Rev. Lett.* **93** 255501
[26] Pérez-Castañeda T, Jiménez-Riobóo R J, and Ramos M A 2014 *Phys. Rev. Lett.* **112** 165901
[27] Pérez-Castañeda T, Rodríguez-Tinoco C, Rodríguez-Viejo J, and Ramos M A 2014 *Proceedings of the National Academy of Sciences of the United States of America* **111** 11275
[28] Yu H B, Gao L, Gao J Q, and Samwer K 2024 *Natl. Sci. Rev.* **11** nwae091
[29] Zella L, Moon J, and Egami T 2024 *Nat. Commun.* **15** 1358
[30] Wang B, Wang L J, Shang B S, Gao X Q, Yang Y, Bai H Y, Pan M X, Wang W H, and Guan P F 2020 *Acta Mater.* **195** 611
[31] Zella L, Moon J, Keffer D, and Egami T 2022 *Acta Mater.* **239** 118254
[32] Tong H and Xu N 2014 *Phys. Rev. E* **90** 010401
[33] Wang L, Ninarello A, Guan P, Berthier L, Szamel G, and Flenner E 2019 *Nat. Commun.* **10** 26
[34] Liu C and Fan Y 2021 *Phys. Rev. Lett.* **127** 215502
[35] Schoenholz S S, Cubuk E D, Sussman D M, Kaxiras E, and Liu A J 2016 *Nat. Phys.* **12** 469
[36] Wu Y, Xu B, Zhang X, and Guan P 2023 *Acta Mater.* **247** 118741
[37] Song K, Zhao R, Liu J *et al.* 2024 *Nat. Commun.* **15** 10208
[38] Novelli P, Meanti G, Buigues P J, Rosasco L, Parrinello M, Pontil M, and Bonati L 2025 *npj Comput. Mater.* **11** 293